Integration of reversible solid oxide cells with methane synthesis (ReSOC-MS) in grid stabilization

Chen, Bin; Hajimolana, Yashar S.; Venkataraman, Vikrant; Ni, Meng; Aravind, P. V.

DOI
10.1016/j.egypro.2019.01.479

Publication date
2019

Document Version
Final published version

Published in
Energy Procedia

Available online at www.sciencedirect.com

ScienceDirect

Energy Procedia 158 (2019) 2077–2084

Energy Procedia

www.elsevier.com/locate/procedia

10th International Conference on Applied Energy (ICAE2018), 22-25 August 2018, Hong Kong, China

Integration of Reversible Solid Oxide Cells with methane synthesis (ReSOC-MS) in grid stabilization

Chen Bin[a,b], Yashar S. Hajimolana[a,*], Vikrant Venkataraman[a], Meng Ni[b], P.V.Aravind[a]

[a]*Process and Energy Department, Delft University of Technology, Leeghwaterstraat 44, CA Delft 2628, The Netherlands*
[b]*Building Energy Research Group, Department of Building and Real Estate, The Hong Kong Polytechnic University, Hung Hom, Kowloon, Hong Kong, China*

Abstract

The power to gas process concept is promising for the next generation of grid electricity storage and stabilization technologies. The electricity-driven fuel production can be chosen to be the efficient energy carrier for excessive grid power. Here, a reversible solid oxide cells system integrated with methane synthesis (ReSOC-MS) is proposed for the grid stabilization application at MW class. Besides H_2, CH_4 can be inclusively synthesized at grid surplus conditions as a transportation friendly energy carrier. A control strategy is proposed for this combined system, based on the grid state and H_2 tank state of the system for the normal SOFC mode and SOEC mode operating. Simulation results of these two modes operating demonstrate that the ReSOC-MS can achieve an 85.34% power to gas efficiency at SOEC mode and 46.95% gas to power efficiency at SOFC mode.

Keywords: reversible solid oxide cell; methane synthesis; grid stabilization; hydrogen storage; dynamic simulation; power control strategy

* Corresponding author. Tel.: +31 (0)6 82355110; fax: +31 (0)6 82355110.
E-mail address: S.Hajimolana-1@tudelft.nl

1. Introduction

The increasing penetration of renewable energy into grid is driving great interests in grid stabilization technologies due to the intermittent nature of renewable power plants such as wind, solar, tidal and etc., that totally accounts for 22.8% of electricity generation according to the European Commission's energy statistical report [1] Grid energy storage technologies mainly ranging from electrochemical methods (battery, capacitor), mechanical methods

10.1016/j.egypro.2019.01.479

(compressed air, flywheel) to thermal storage [2], are required to own favorable characters such as high roundtrip efficiency, low capital cost and fast response [3]. Reversible Solid Oxide Cell (ReSOC) is considered to be a promising choice for the peak shifting, attributed to the high efficiency at its operating temperature (600–900ºC), which is preferable in large scale energy storage. The operating of ReSOC at electrolysis cell (EC mode) can convert steam to hydrogen (or carbon dioxide to carbon monoxide), as a form of chemical energy that stores the redundant electricity at peak hours of the intermittent renewable grid [4]; while at off-peak ReSOC is operated as fuel cell(SOFC mode), injecting electricity to the grid using the pre-stored fuel gas with a higher efficiency than the traditional fuel turbine (~40%) [5]. CO_2 methanation using the H_2 produced in ReSOC [6] is considered as an attractive option since it can be operated at moderate conditions with well commercialized large scale chemical process that uses low cost Ni-based catalyst and such as the adiabatic fixed bed process system (e.g. Lurgi and TREMP); cooled fixed-bed (e.g. Linde) and other fluid bed methanation processes [7]. Besides, the CO_2 methanation process can serve to recycle the CO_2 from various carbon capture and storage (CCS) technologies. As such, the CO_2 emission can be alleviated by increasing the penetration of sustainable hydrocarbon fuels. Therefore, this paper proposed a reversible solid oxide cells with methane synthesis system (ReSOC-MS), which integrates the CO_2 methanation subsystem with ReSOC sub-system that can be operated at the SOEC mode and at SOFC mode to balance the grid.

2. Overview of system operation and model development

The ReSOC-MS system consists of two sub-systems as depicted in Fig. 1: the ReSOC subsystem and methanation subsystem, connected by the H_2 supply stream (***S16***) and the water recycle stream (***S18***). The grid is linked with the ReSOC subsystem with the electricity input (W_{elec_FC}) or output (W_{elec_EC}), depending on different states of the electricity grid. A proper PID controller is employed to regulate the power output of ReSOC by manipulating the current density of the ReSOC.

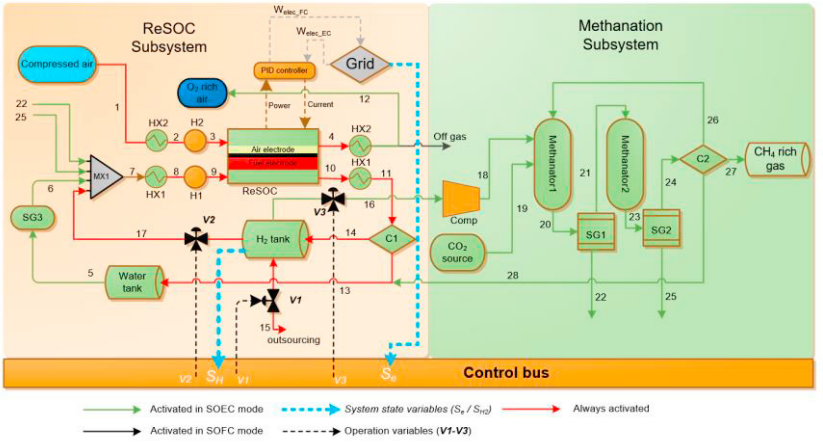

Fig. 1. The overall system schematic of the ReSOC-MS system

In case of real-time grid electricity surplus, the ReSOC would be operated under SOEC mode at 600°C with the reaction occurring in ReSOC block:

$$2H_2O = O_2 + 2H_2 \qquad \Delta H = 493 \text{ kJ mol}^{-1} \tag{1}$$

The ReSOC subsystem can utilize the redundant electricity (W_{elec_EC}) from grid to electrolyze the steam-rich stream (the mixture of ***S5***, ***S6***, ***S22***, ***S25*** and ***S17***) to produce H_2. The produced H_2 in ***S10*** is going to be stored in the H_2 tank via ***S14***, after proper heat recuperation (***S11***) and splitting from unused steam at Condenser (**C1**) by condensing. The stored H_2 can be utilized by the ReSOC via ***S17*** to generate electricity so as to mitigate the grid shortage when the ReSOC operated at SOFC mode with the reaction (Eq. 1) reversed. The compressed air is used as oxygen source in the SOFC mode and the O_2 rich gas can be generated at the SOEC mode. Heat exchanger ***HX2*** and Heat (***H2***) is also designed to control the inlet temperature of air (***S3***) to be consistent of fuel stream inlet of ReSOC. The cumulative

storage of H_2 would be further transferred to the Methanation subsystem for the synthesis of methane via Sabatier reaction:

$$CO_2 + 4H_2 = CH_4 + 2H_2O \qquad \Delta H\text{=-164 kJ mol}^{-1} \tag{2}$$

The methanation subsystem consisted of two Sabatier reactors with inter-stage cooling. The H_2 sources from the H_2 tank would be firstly adiabatically compressed to the working pressure (10 bar, ***S18***), and mixed with the compressed CO_2 (***S19***) source and the recycled product gas (***S26***). The inlet gas temperature of the first stage *Methanator1* is fixed at 250°C. The condenser ***C2*** will condense the steam contained in ***S24*** to liquid water (***S28***) and stored the CH_4 rich gas (***S27***) with 10% recycled to *Methanator1*.

The control bus component is responsible for the timely control of gas streams flux so that the system can switch between SOFC mode and SOEC mode along with the change of grid state. The system state is represented by two variables: the grid state S_e and the H_2 tank state S_{H_2} that respectively representing the dimensionless grid electricity surplus/shortage (-1.0~1.0, normalized to 5 MW) and the filling degree of the H_2 tank as shown in Fig. 1. A control strategy based on these two state variables would be implemented into the control bus to regulate three pipe valves for streams by three operating signals (***V1-V3***) with capability of state-dependent. During normal SOEC and SOFC modes (no need for outsourcing via ***V1***), the openings of ***V1-V3*** can be controlled by:

SOFC mode: $\boldsymbol{V1} = 0; \boldsymbol{V2} = S_e; \boldsymbol{V3} = 0;$

SOEC mode: $\boldsymbol{V1} = 0; \boldsymbol{V2} = 0.05; \boldsymbol{V3} = S_{H_2} - (S_e + 2) / 4\ (Methanation)$

Please note that more dedicated control strategies at complicated state cases of (S_e and S_{H_2}) can be freely proposed and implemented to the control bus block, which would be the focus of our future work.

Above all, this system is modelled in the process simulation platform OpenModelica at the nominal operating conditions as Table 1.

Table 1. The nominal operation conditions of the system.

Name	Parameters
Heat exchanger (***HX1-2***)	Effectiveness: 0.85
Heaters (***H1-2***)	Outlet temperature: 600°C
Steam generator (***SG3***)	Outlet temperature: 100°C
Compressed air	Flowrate: 0.5 mol s^{-1} at SOEC; $10S_e$ mol s^{-1} at SOFC; Pressure: 1 bar
Water tank	25°C, 1 bar
H_2 tank	25°C, 1 bar, Capacity: 6000 mol H_2
Maximum valve flowrate through ***V2*** and ***V3***	55 mol s^{-1}; 20 mol s^{-1}
Condenser (***C1***)	Condensing temperature: 100°C
PID controller	kp=0.0001; ki=1; kd=1

2.1. ReSOC subsystem model

A zero-dimensional dynamic model for the ReSOC performance is developed in this model based on transfer functions of the partial pressure of participating gas species. Various loss effects on the dynamic performance of ReSOC (Ohmic loss, activation loss, concentration loss) are taken consideration of. Fig. 2 shows the mathematical model of the ReSOC component with three input ports and three output ports interfaced to other auxiliary components in the ReSOC system [8,9]. The deduction of this mathematical model starts from the assumed ideal gas behaviour of gas species inside the ReSOC gas channels, taking H_2 as example:

$$P_{H_2}V = n_{H_2}RT\ ;\ q_{H_2} = \frac{dn_{H_2}}{dt} \tag{3-4}$$

The q_{H_2} is defined as the molar flow rate of hydrogen within the channel, thus the derivative of P_{H_2} can be expressed as:

$$\frac{dP_{H_2}}{dt} = \frac{RT}{V} q_{H_2} \tag{5}$$

As the q_{H_2} should be conserved in terms of influx, outflux and electrochemical reaction term within the channel, we have:

$$\frac{dP_{H_2}}{dt} = \frac{RT}{V}\left(q_{H_2}^{in} - q_{H_2}^{out} - q_{H_2}^{r}\right) \tag{6}$$

of which the $q_{H_2}^{r}$ represents the electrochemical reacted amount of H_2 in unit of mol s^{-1}.

$$\frac{q_{H_2}^{out}}{P_{H_2}} = K_{H_2} \tag{8}$$

The K_{H_2} is defined as the valve molar constant of hydrogen, the value of which can be found in Table 2 along with K_{O_2} and K_{H_2O} [10]. Rearranged and taking Laplace transform of Eq. 6, the transfer function of the state variable P_{H_2} can be obtained:

$$P_{H_2}(s) = \frac{1/K_{H_2}}{1+\tau_{H_2}s}(q_{H_2}^{in} - q_{H_2}^{r}) \tag{9}$$

Similarly, for P_{H_2O} and P_{O_2}:

$$P_{H_2O}(s) = \frac{1/K_{H_2O}}{1+\tau_{H_2O}s}\left(q_{H_2O}^{in} + q_{H_2}^{r}\right) \tag{10}$$

$$P_{O_2}(s) = \frac{1/K_{O_2}}{1+\tau_{O_2}s}(q_{O_2}^{in} - 0.5 \times q_{H_2}^{r}) \tag{11}$$

, where the time response time for each flow is calculated as:

$$\tau_{H_2} = \frac{\upsilon}{K_{H_2}RT}, \tau_{H_2O} = \frac{\upsilon}{K_{H_2O}RT} \; and \; \tau_{O_2} = \frac{\upsilon}{K_{O_2}RT} \tag{12-14}$$

The transfer functions for the outlet partial pressure (Eq. 9-11) are implemented together with the blocks of electrochemical model for the calculation of cell voltage and overpotentials [10,11]:

Cell voltage:

$$V_{soc} = E_0 + \frac{RT}{2F} ln(\frac{P_{H_2}\sqrt{P_{H_2O}}}{P_{H_2O}}) - \eta_{ohm} - \eta_{act,i} - \eta_{act,i} - \eta_{conc} \tag{15}$$

Ohmic overpotential:

$$\eta_{ohm} = i \times \delta \times 2.99 \times 10^{-5} exp(10300/T) \tag{16}$$

Activation overpotential:

$$\eta_{act,i} = \frac{RT}{nF} l\, n\left(\frac{j}{2j_{0,i}} + \sqrt{\left(\frac{j}{2j_{0,i}}\right)^2 + 1}\right);\ \mathrm{j}_{0,i} = \gamma_i \exp(\frac{-E_{act,i}}{RT}) \tag{17-18}$$

Concentration overpotential:

$$\eta_{conc} = \begin{cases} -\frac{RT}{nF} ln\left(1 - \frac{j}{j_{limit}}\right), & SOFC\ mode \\ \frac{RT}{nF} ln\left(1 - \frac{j}{j_{limit}}\right), & SOEC\ mode \end{cases} \tag{19}$$

, where the δ is the thickness of the electrolyte layer. The Ohmic loss is assumed all from the charge transport in the electrolyte layer as a reasonable simplification [12], $j_{0,i}$ is the exchange current densities of air electrode ($i = a$) and fuel electrode ($i = f$). γ_i is pre-exponential factor. j_{limit} is the limiting current density.

Table 2. ReSOC stack parameters used in the model [10].

Name	Parameters
Operating temperature, T (°C)	600
Operating pressure, P (bar)	1
Standard equilibrium potential, E_0 (V)	1.18
Pre-exponential factor for air electrode exchange current density, γ_a (A m^{-2})	2.051×10^9
Pre-exponential factor for fuel electrode exchange current density, γ_f (A m^{-2})	1.344×10^{10}
Activation energy for air electrode, $E_{act,a}$ (J mol^{-1})	1.2×10^5
Activation energy for fuel electrode, $E_{act,f}$ (J mol^{-1})	1.0×10^5
Electrolyte thickness, δ (μm)	50
Number of cells in series in the stack, N	64000
Single cells active area, cm^2	100
Limiting current density of the ReSOC j_{limit} (A m^{-2})	9000 at SOFC [8]; -10000 at SOEC [10]
Valve molar constant for hydrogen, K_{H_2}, kmol s^{-1} atm^{-1})	8.43×10^{-4}
Valve molar constant for water, K_{H_2O}, kmol s^{-1} atm^{-1})	2.52×10^{-3}

Valve molar constant for oxygen, K_{O_2}, kmol s^{-1} atm^{-1})	2.81×10^{-4}

2.2. Methanation subsystem model

The methanation unit of the whole system is responsible for the synthesis of methane using the H_2 stored in the compressed tank (25 °C, 1 bar), that is accumulatively produced by the ReSOC in mode of SOEC. The process is based on two identical adiabatic fixed-bed methanators (*Methanator1* and *Methanator2*) with intercooling learned from the exemplary 3-staged TREMP methanation process developed by Haldor Topsøe™ [13]. The main reaction occurring in the two methanators is the so-called CO_2 methanation reaction (see Eq. 2). The feeding gas temperature of *Methantor1* are controlled at 250 °C at which the favorableness of kinetics and thermodynamics of the CH_4 production could be balanced. Preheating the H_2 stream and recycling 10% of the outlet gas of *Methanator2* at the condenser (***C2***) are the two measures for the inlet temperature control of *Methanator1*. Before *Methanator2*, ***SG1*** is used to cool down the flue gas of *Methanator1* to 400°C before entering *Methanator2*. The design parameters of the methanators and the operating parameters of based case of the methantion process are referred to Table 3 and 4. The CO_2 methanation kinetics over Ni/Al_2O_3 are adopted from Koschany's power law equation deduced from their catalyst characterization results [14] considering the inhibition effects of adsorbed hydroxyl:

$$r = k \cdot \frac{p_{H_2}^{n_{H_2}} p_{CO_2}^{n_{CO_2}}}{1+K_{OH}\frac{p_{H_2O}}{p_{H_2}^{1/2}}} \left(1 - \frac{p_{CH_4}\, p_{H_2O}^2}{p_{H_2}^4\, p_{CO_2}\, K_{eq}}\right) \tag{20}$$

, of which the r represents the volume reaction rate of CO_2 methanation in mol s^{-1}m^{-3}. The equilibrium constant K_{eq}:

$$K_{eq} = 137 \cdot T^{-3.998} \cdot \exp\left(\frac{158.7\ \text{kJ mol}^{-1}}{RT}\right) \tag{21}$$

The adsorption constant k is based on the Arrhenius type:

$$k = 6.41 \cdot 10^{-5} \cdot \exp\left(\frac{E_a}{R}\left(\frac{1}{T_{ref}} - \frac{1}{T}\right)\right) \tag{22}$$

And the adsorption constant of hydroxyl is calculated as:

$$K_{OH} = 0.62 \cdot \exp\left(\frac{\Delta H_{OH}}{R}\left(\frac{1}{T_{ref}} - \frac{1}{T}\right)\right) \tag{23}$$

The enthalpy change of hydroxyl adsorption (ΔH_{OH}) is estimated as 22.4 kJ mol^{-1} when T_{ref} is set at 555 K. Using the above mentioned equations, a one-dimensional plug-flow model is developed for the methanator to simulate the reaction process inside the methanator along the axial direction.

Table 3. The design parameters of the methanators.

Working pressure	10 bar
Catalyst type	Ni/Al_2O_3
Catalyst density (ρ_c)	2800 kg mol^{-1}
Bed porosity	0.4
Methanator catalyst loading	3.0 kg
Methanator inner diameter	0.45 m
Methanator length	2.0 m
Space velocity, GSHV (nominal, opening of ***V3*** =1)	6800 h^{-1} (STP)
Inlet gas composition before mixing with recycled gas	H_2:CO_2=4
Inlet gas flowrate before mixing with recycled gas (nominal, opening of ***V3*** =1)	25 mol s^{-1}
Discretized number (N)	400

Table 4. The operating parameters of based case of the methanation process.

Name of components/stream	Parameters	value
H_2 source (***S16***)	Temperature, T_{H2}	25°C
	Pressure, P_{H2} [16]	10 bar
	Maximum flowrate, F_{H2}	20 mol s^{-1}

	Temperature, T_{CO2}	25°C
CO_2 source	Pressure, P_{CO2} [16]	10 bar
	Maximum flowrate, F_{CO2}	5 mol s^{-1}
Steam generator (***S1*** and ***S2***)	Temperature of feed-water	25°C
	Outlet steam temperature	100°C
Methanator1	Inlet temperature	250°C
Methanator2	Inlet temperature [17]	400°C
Condenser (***C2***)	Recycle ratio	10%
	Outlet temperature at 10 bar [18]	177 °C
Compressor (***COMP***)	Compressing ratio	10
	Isentropic efficiency	85%

3. Operation results

To analyse the performance of this system, two simulation cases are conducted. Stationary S_e input lasting for 1000s is assigned to both the SOEC case and SOFC case. The initial conditions are the SOFC case with 1 MW input from the grid ($S_e = 0.25, S_{H_2} = 0.5$) and the SOEC case with 2 MW to be output ($S_e = -0.4, S_{H_2} = 0.5$). The initial H_2 tank state are assumed to be 50% filled ($S_{H_2} = 0.5$) which in real operation the state of the tank would generally be close to.

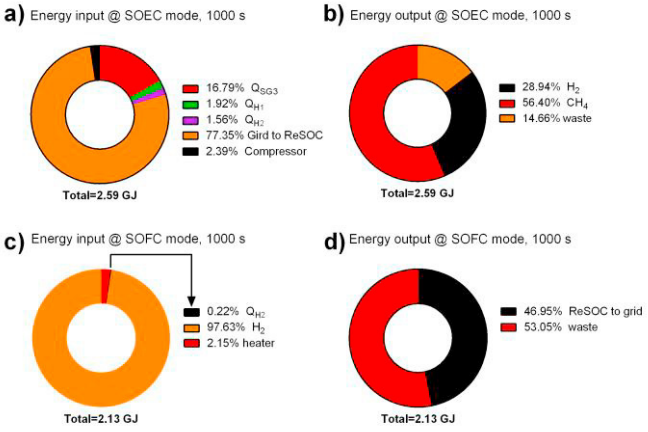

Fig. 8. Accumulative energy input and output of the system for the SOFC case and SOEC case for 1000s

Fig. 8 compares the energy input and output for both cases. At t=1000s of SOEC case (Fig.8a), an average 2.59 GJ power was input to the system via the grid to the ReSOC stack, electricity consumed by 3 heaters (Q_{H1}, Q_{H2} and Q_{SG1}) and the compressor. The grid to the ReSOC stack power, namely the electrolysis energy consumption inside the stack accounts for 77.35%. Regarding the energy output (Fig. 8b), it can be seen that 14.66% was wasted and 56.4% stored in the CH_4 and 28.94% stored in the H_2 produced. This power to gas efficiency (85.34%) is quite high since the SOEC is operated at 1.44 V which is close to the thermal-neutral voltage (approximately 1.29 V at 800°C). In the SOFC case, the total energy 2.13 GJ mostly originates from the high heat value (HHV) of the consumed H_2 (97.63%), while still slight amount of electricity should be needed for other components. The total energy power is 53.05% wasted due to the SOFC operated at 0.71 V at which the electrical efficiency is less than 70%. The simulation results of the two case operating are summarized in Table 5.

Table 5. Summary of the simulation cases.

Performance parameters	SOEC mode	SOFC mode
Average methane production rate	0.97 mol s^{-1}	—

H_2 consumption (<0)/production (>0)	3.28 mol s^{-1}	-7.27 mol s^{-1}
Initial H_2 tank state, S_{H2}	0.5	0.5
Simulated operation time, s	1000 s	1000 s
Constant grid power input/output, MW (grid state, S_e)	-2 MW ($S_e = -0.4$)	1 MW ($S_e = 0.25$)
Operating Voltage of SOC, V_{SOC} and current density	1.44 V -2307.9 A m^{-2}	0.71 V 2338.6 A m^{-2}

4. Conclusions

This paper proposes a combined system integrating ReSOC with CO_2 methanation process for the grid electricity storage at a scale of MW class. The simulation results of stationary tests show that the combined system can achieve an 85.34% power to gas efficiency when operated at stationary grid condition (2 MW, SOEC mode at 1.44 V) with a CH_4 yield of 0.97 mol s^{-1}, viz. 68.1% CO_2 conversion ratio for 1000s operation. When operated at SOFC mode of 1 MW, the ReSOC-MS system achieves a gas to power efficiency of 46.95% at 0.71V.

Acknowledgment

This project BALANCE is funded by H2020 under the grant agreement 731224.

References

[1] European Union energy in figures statistical pocketbook 2017. Publications Office of the European Union; 2017.
[2] Eyer J, Corey G. Energy storage for the electricity grid: Benefits and market potential assessment guide. Sandia Natl Lab 2010;20:5.
[3] Hittingera E,Whitacreab JF, Apt J. What properties of grid energy storage are most valuable? J Power Sources 2012;206:436–49.
[4] Zabihian F, Fung A. A review on modeling of hybrid solid oxide fuel cell systems. Int J Eng 2009;3:85–119.
[5] Chen B, Xu H, Zhang H, Tan P, Cai W, Ni M. A novel design of solid oxide electrolyser integrated with magnesium hydride bed for hydrogen generation and storage –A dynamic simulation study, Appl. Energy. 200 (2017) 260–272.
[6] Chen B, Xu H, Sun Q, Zhang H, Tan P, Cai W, He W, Ni M, Syngas/power cogeneration from proton conducting solid oxide fuel cells assisted by dry methane reforming: A thermal-electrochemical modelling study, Energy Convers. Manag. 167 (2018) 37–44.
[7] Rönsch S, Schneider J, Matthischke S, Schlüter M, Götz M, Lefebvre J, et al. Review on methanation - From fundamentals to current projects. Fuel 2016;166:276–96.
[8] Mary N, Augustine C, Joseph S, Heartson S. Dynamic Modeling and Fuzzy Control for Solid Oxide Fuel Cell (SOFC). Int J Adv Res Electr Electron Instrum Eng 2016;5:2278–8875.
[9] Padulles J, Ault GW, Mcdonald JR. An integrated SOFC plant dynamic model for power systems simulation. J Power Sources 2000;86:495–500.
[10] Ni M, Leung MKH, Leung DYC. Energy and exergy analysis of hydrogen production by solid oxide steam electrolyzer plant. Int J Hydrogen Energy 2007;32:4648–60.
[11] Ni M, Leung MKH, Leung DYC. A modeling study on concentration overpotentials of a reversible solid oxide fuel cell. J Power Sources 2006;163:460–6.
[12] Ni M, Leung MKM, Leung DYC. Parametric study of solid oxide steam electrolyzer for hydrogen production. Int J Hydrogen Energy 2007;32:2305–13.
[13] Simakov DSA. Renewable Synthetic Fuels and Chemicals from Carbon Dioxide: Fundamentals, Catalysis, Design Considerations and Technological Challenges. Springer; 2017.
[14] Koschany F, Schlereth D, Hinrichsen O. On the kinetics of the methanation of carbon dioxide on coprecipitated $NiAl(O)_x$. Appl Catal B Environ 2016;181:504–16.
[15] Schlereth D, Hinrichsen O. A fixed-bed reactor modeling study on the methanation of CO_2. Chem Eng Res

Des 2014;92:702–12.
[16] Froment GF. Methane Steam Reforming , Methanation and Water-Gas Shift : 1 . Intrinsic Kinetics 1989;35:88–96.
[17] Rostrup-Nielsen JR, Pedersen K, Sehested J. High temperature methanation. Sintering and structure sensitivity. Appl Catal A Gen 2007;330:134–8.
[18] Wagner W, Kretzschmar H-J. IAPWS industrial formulation 1997 for the thermodynamic properties of water and steam. Int Steam Tables Prop Water Steam Based Ind Formul IAPWS-IF97 2008:7–150.